

# Voltage-controlled colossal magnetoresistance in manganite/normal-metal heterostructures

M. Ziese and S. Sena

*Department of Physics, University of Sheffield, Sheffield S3 7RH, United Kingdom*

C. Shearwood

*Department of Electronic and Electrical Engineering, University of Sheffield, Sheffield S1 3JD, United Kingdom*

H. J. Blythe, M. R. J. Gibbs, and G. A. Gehring

*Department of Physics, University of Sheffield, Sheffield S3 7RH, United Kingdom*

(Received 18 September 1997)

It is well established that the resistivity of the manganites is a strong function of the magnetization. Near the ferromagnetic ordering temperature, colossal changes in the resistivity are seen in applied fields of several Tesla; such fields are too large for a number of potential applications. An alternative approach is to change the state of magnetization by injecting spin polarized carriers into manganite/classical ferromagnet heterostructures. In this work, results on manganite/normal-metal heterostructures in current perpendicular-to-plane geometry are reported. We observe a colossal magnetoresistance in fields of the order of 1 T which we attribute to magnetic interface scattering. The magnitude of this magnetoresistive effect can be controlled by the applied voltage, i.e., the heterostructures act as magnetic sensors with variable sensitivity. Implications of the interface resistance on spin injection from classical ferromagnets into manganites are discussed. [S0163-1829(98)00206-9]

## I. INTRODUCTION

The manganites show colossal magnetoresistance effects of different origin. Near the magnetic ordering temperature the application of strong magnetic fields of the order of several Tesla leads to huge resistance changes in the bulk,<sup>1</sup> whereas relatively small fields induce a considerable magnetoresistance in samples with grain boundaries at low temperatures.<sup>2</sup> However, these effects do not provide a physical basis for potential applications of the manganites at room temperature in small magnetic fields, e.g., as magnetic switches. To overcome these problems our group has recently developed a device that allows control of the switching field by polarized carrier injection in a manganite/permalloy heterostructure.<sup>3</sup> The performance of these devices crucially depends on the interface quality.

In this work the properties of manganite/normal-metal interfaces are investigated. Current perpendicular-to-plane (CPP) measurements on manganite/normal-metal heterostructures show the existence of a large boundary resistance. We report the observation of a voltage controlled colossal magnetoresistance associated with the manganite/normal-metal interface, thereby opening up new routes to potential applications. Spin injection from a nickel layer into  $\text{La}_{0.7}\text{Ca}_{0.3}\text{MnO}_3$  could not be observed, since the transport properties of these devices are dominated by the interface resistance.

## II. DEVICE FABRICATION AND EXPERIMENTAL DETAILS

$\text{La}_{0.7}\text{Ca}_{0.3}\text{MnO}_3$  films were grown by laser ablation (XeCl, 308 nm) from a stoichiometric target at an oxygen partial pressure of 100 mTorr and a substrate temperature of

720 °C. High quality epitaxial films were produced by this route on  $\text{LaAlO}_3$  and  $\text{SrTiO}_3$  substrates with an as-deposited Curie temperature  $T_C$  of 230 K and a resistivity maximum in zero field  $T_R$  of 235 K. A postannealing treatment for 2 h at 950 °C in flowing oxygen yields films with  $T_C$  of 280 K and  $T_R$  of 290 K. In Figs. 1(a) and 1(b) the resistivity of an

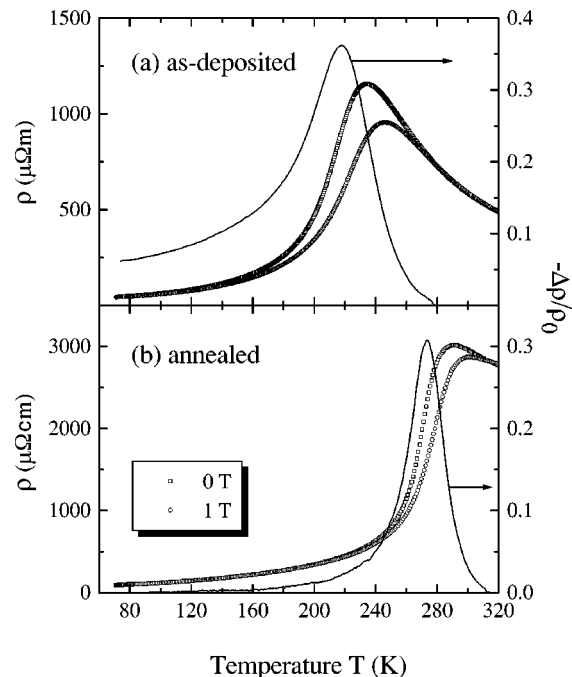


FIG. 1. Resistivity and magnetoresistance  $\Delta\rho/\rho_0$  of an (a) as-deposited and (b) annealed  $\text{La}_{0.7}\text{Ca}_{0.3}\text{MnO}_3$  film as a function of temperature in zero field and 1 T applied parallel to the film surface. Note the different scales of the upper and lower panel.

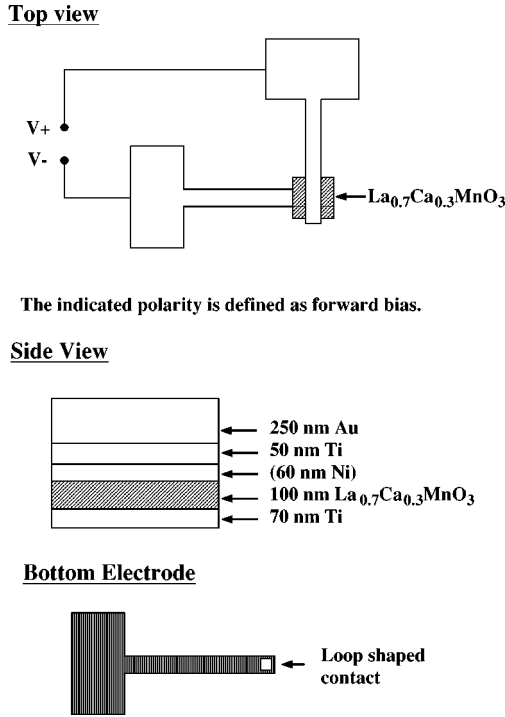


FIG. 2. Schematic drawing of the heterostructure.

as-deposited and an annealed  $\text{La}_{0.7}\text{Ca}_{0.3}\text{MnO}_3$  film on  $\text{LaAlO}_3$  are shown as a function of temperature in zero field and a magnetic field of 1 T applied parallel to the film. The high Curie temperatures of the as-deposited as well as the annealed films prove the high quality of our samples. The resistivities  $\rho$  and the magnetoresistance at 1 T,  $\Delta\rho/\rho_0$ , given by

$$\Delta\rho/\rho_0 = [\rho(1\text{ T}) - \rho(0\text{ T})]/\rho(0\text{ T}), \quad (1)$$

are in agreement with published values.<sup>1</sup>

Such growth conditions, however, are an intrinsic obstacle in the fabrication process of normal-metal/manganite/normal-metal heterostructures in CPP geometry since the high substrate temperature at a relatively high oxygen partial pressure limits the choice of metals suitable as bottom electrode. Furthermore, epitaxy is lost if  $\text{La}_{0.7}\text{Ca}_{0.3}\text{MnO}_3$  films are grown on a metal layer, thus resulting in polycrystalline  $\text{La}_{0.7}\text{Ca}_{0.3}\text{MnO}_3$  films of low quality.

In our devices, titanium was chosen for the bottom electrode since it is easily deposited, adheres strongly to the substrate, and forms a conducting oxide.<sup>4</sup> This bottom contact was etched into a loop shape, Fig. 2, so as to maximize the contact area between the  $\text{La}_{0.7}\text{Ca}_{0.3}\text{MnO}_3$  film and the substrate and thus obtain as good an epitaxial growth as possible.

Four devices on  $\text{LaAlO}_3$  substrates have been realized using photolithographic techniques. First a 70 nm titanium layer was deposited on a  $\text{LaAlO}_3$  substrate and etched into a T-shaped bottom contact, Fig. 2. In the next step, a 100 nm  $\text{La}_{0.7}\text{Ca}_{0.3}\text{MnO}_3$  film was deposited by laser ablation at the aforementioned growth parameters. For two of the devices, a 60 nm nickel layer was deposited onto the  $\text{La}_{0.7}\text{Ca}_{0.3}\text{MnO}_3$  film. The  $\text{La}_{0.7}\text{Ca}_{0.3}\text{MnO}_3$  layer (and the nickel layer where applicable) are patterned into small squares for the CPP mea-

TABLE I. Parameters of the CPP devices on  $\text{LaAlO}_3$ .  $T_R$  denotes the temperature of the zero field resistance maximum in the limit of high applied voltages.

Sample	Multilayer	Contact area	$T_R$
A	Ti/ $\text{La}_{0.7}\text{Ca}_{0.3}\text{MnO}_3$ /Ti	$37\ \mu\text{m} \times 37\ \mu\text{m}$	175 K
B	Ti/ $\text{La}_{0.7}\text{Ca}_{0.3}\text{MnO}_3$ /Ti	$70\ \mu\text{m} \times 70\ \mu\text{m}$	108 K
C	Ti/Ni/ $\text{La}_{0.7}\text{Ca}_{0.3}\text{MnO}_3$ /Ti	$37\ \mu\text{m} \times 37\ \mu\text{m}$	126 K
D	Ti/Ni/ $\text{La}_{0.7}\text{Ca}_{0.3}\text{MnO}_3$ /Ti	$70\ \mu\text{m} \times 70\ \mu\text{m}$	231 K

surements and rectangular bridges for current-in-plane (CIP) measurements. Finally, another 50 nm titanium layer and a 250 nm gold layer were evaporated and the top electrodes were patterned and bonded with gold wires. The contact areas, i.e., the effective overlap between top and bottom electrode, were  $37\ \mu\text{m} \times 37\ \mu\text{m}$  and  $70\ \mu\text{m} \times 70\ \mu\text{m}$  for small and large geometries, respectively. The titanium loop was approximately  $50\ \mu\text{m} \times 50\ \mu\text{m}$  and 4  $\mu\text{m}$  in width and  $98\ \mu\text{m} \times 98\ \mu\text{m}$  and 7  $\mu\text{m}$  in width, respectively. The in-plane bridge had a size of  $890\ \mu\text{m} \times 185\ \mu\text{m}$  and was bonded with gold wires onto titanium/gold squares forming the contact areas. The parameters of the CPP devices are summarized in Table I.

Resistance measurements were performed in standard four-point configuration. However, each pair of voltage and current leads was bonded to a single contact, thus sampling the interface resistance between contact and manganite as well as the manganite bulk resistance. This contact configu-

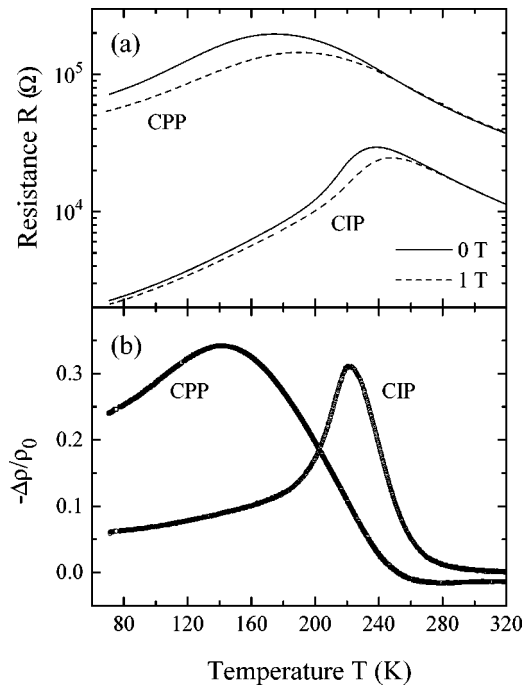


FIG. 3. (a) Resistance in current perpendicular-to-plane (CPP) geometry of a  $\text{Ti}/\text{La}_{0.7}\text{Ca}_{0.3}\text{MnO}_3/\text{Ti}$  heterostructure, sample A, and current-in-plane (CIP) geometry of a  $\text{Ti}/\text{La}_{0.7}\text{Ca}_{0.3}\text{MnO}_3/\text{Ti}$  bridge. The resistance was measured in zero field and 1 T applied parallel to the layers at a constant voltage of 5 V in the CPP geometry and a constant current of 100  $\mu\text{A}$  in the CIP geometry, respectively. (b) Magnetoresistance ratio  $\Delta\rho/\rho_0$  of the samples of Fig. 2(a) in an applied field of 1 T.

ration is common for measurements on current perpendicular-to-plane (CPP) devices<sup>5</sup> and was adopted here for current-in-plane (CIP) samples to allow for a better comparison to be made.

### III. RESULTS AND DISCUSSION

#### A. Interface resistance

Figure 3(a) shows the resistance in CPP geometry of the trilayer Ti/La<sub>0.7</sub>Ca<sub>0.3</sub>MnO<sub>3</sub>/Ti, sample A, in comparison to the resistance in CIP geometry of a Ti/La<sub>0.7</sub>Ca<sub>0.3</sub>MnO<sub>3</sub>/Ti bridge realized on the same substrate. The measurements were performed in zero field and a field of 1 T applied parallel to the layers at a fixed voltage of 5 V in CPP geometry and a fixed current of 100  $\mu$ A in CIP geometry, respectively. The magnetoresistance at 1 T,  $\Delta\rho/\rho_0$ , is shown in Fig. 3(b) for both samples.

The in-plane Ti/La<sub>0.7</sub>Ca<sub>0.3</sub>MnO<sub>3</sub>/Ti bridge shows a zero field resistance maximum at 236 K; this is typical for our as-deposited films. The Ti/La<sub>0.7</sub>Ca<sub>0.3</sub>MnO<sub>3</sub>/Ti trilayer shows a zero field  $T_R$  at the lower temperature of 175 K and a comparatively broad transition. However, the maximum values of  $-\Delta\rho/\rho_0$  of about 35% are similar for both samples.

The striking feature of the measurements is the large magnitude of the CPP resistance compared to the CIP resistance. This might be illustrated by a simple example. At 236 K in zero field we find  $R_{\text{CIP}} \approx 30$  k $\Omega$  and therefore a resistivity  $\rho_{\text{CIP}} \approx 6 \times 10^{-4}$   $\Omega\text{m}$ ; this is in agreement with literature values.<sup>6</sup> Therefore a CPP resistance  $R_{\text{CPP}} \approx 44$  m $\Omega$  is expected in our geometry. However, experimentally we find  $R_{\text{CPP}} \approx 100$  k $\Omega$  at 5 V and 236 K, i.e., a value more than six orders of magnitude larger than expected.

This observation indicates the relevance of an interface resistance, i.e., the measured resistance  $R$  consists of a boundary resistance  $\rho_{\square}/A_{\square}$  as well as a bulk resistance  $\rho l/A$  giving

$$R = 2\rho_{\square}/A_{\square} + \rho l/A. \quad (2)$$

$\rho_{\square}$  denotes the areal interface resistivity,  $A_{\square}$  the interface area,  $\rho$  the bulk resistivity,  $l$  the length of the sample, and  $A$  the sample cross section; for CPP geometries we have  $A = A_{\square}$ . We assume that the two interface resistances are equal.

If we assume that the CPP resistance is entirely due to the boundary resistance, we obtain  $\rho_{\square} = 7 \times 10^{-5}$   $\Omega\text{m}^2$  at 236 K and an in-plane resistance at 5 V

$$R_{\text{CIP}} = 4 \text{ k}\Omega + \rho l/A. \quad (3)$$

The interface resistance model is therefore in agreement with the measured resistances.

As will be shown in Sec. III C the interface resistivity  $\rho_{\square}$  is a strong function of the applied voltage; thus the CIP resistance should contain a nonlinear component according to Eq. (2). This is indeed found.

#### B. Voltage controlled magnetoresistance

In the previous section it was shown that the resistance measured in CPP geometry is due to an interface resistance

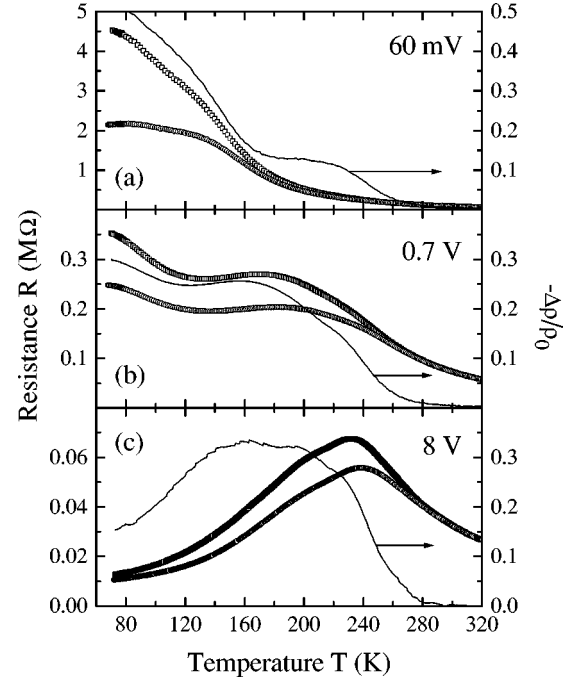


FIG. 4. CPP resistance (open symbols) at 0 T ( $\square$ ) and 1 T ( $\circ$ ) applied parallel to the layers and magnetoresistance  $\Delta\rho/\rho_0$  (solid lines) at 1 T of a Ti/Ni/La<sub>0.7</sub>Ca<sub>0.3</sub>MnO<sub>3</sub>/Ti heterostructure, sample D, for different applied voltages: (a) 60 mV, (b) 0.7 V, (c) 8 V.

at the manganite/normal-metal boundary. In this section we discuss the voltage dependence of the interface resistance.

In Figs. 4(a)–4(c) both the CPP resistance and magnetoresistance  $\Delta\rho/\rho_0$  of a Ti/Ni/La<sub>0.7</sub>Ca<sub>0.3</sub>MnO<sub>3</sub>/Ti multilayer, sample D, are shown as a function of temperature in zero field and with 1 T applied parallel to the layers. The measurements were performed at fixed voltages over the sample of 60 mV [Fig. 4(a)], 0.7 V [Fig. 4(b)], and 8 V [Fig. 4(c)], respectively. All measurements show a considerable magnetoresistance  $\Delta\rho/\rho_0$ . However, the temperature of maximum magnetoresistance  $T_R$  strongly depends on the applied voltage. The measurements indicate that the magnetoresistance consists of two contributions, i.e., a low-temperature part that increases with decreasing temperature and decreases with increasing voltage and a high-temperature contribution that increases with increasing voltage. We stress that this behavior is not related to the nickel layer but is seen in all samples. Note that the zero field CPP resistance measured at high voltages has a maximum at 231 K, i.e., near the Curie temperature of our as-deposited La<sub>0.7</sub>Ca<sub>0.3</sub>MnO<sub>3</sub> films.

We interpret these observations as follows. The manganite/normal-metal interface forms a highly resistive boundary due to scattering from magnetic disorder. The application of a magnetic field suppresses the magnetic fluctuations and leads to a large negative magnetoresistance. For higher voltages, new conduction channels open up and lead to a decrease in resistance. The multilayers form a magnetoresistive structure in which the sensitivity of the magnetoresistance can be controlled by the application of a voltage. This can be elegantly seen in Fig. 5 showing the CPP magnetoresistance of a Ti/La<sub>0.7</sub>Ca<sub>0.3</sub>MnO<sub>3</sub>/Ti trilayer, sample B, at 96 K as a function of magnetic field. At high applied

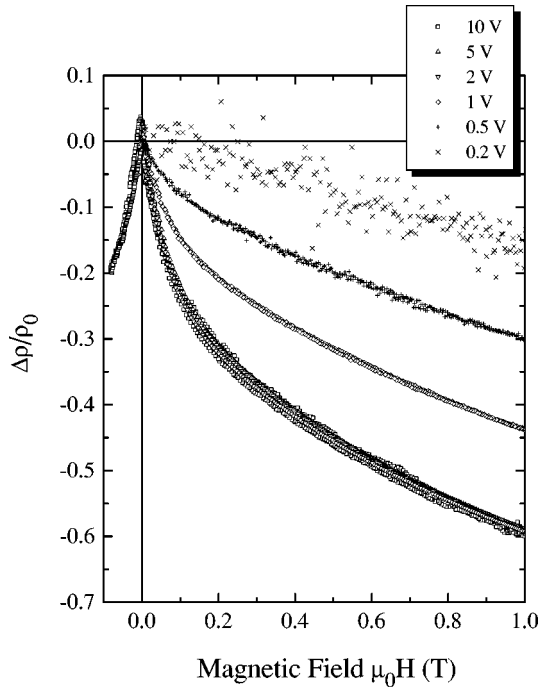


FIG. 5. Magnetoresistance of a Ti/La<sub>0.7</sub>Ca<sub>0.3</sub>MnO<sub>3</sub>/Ti multilayer, sample B, at 96 K and different applied voltages 0.2 V ≤ V ≤ 10 V. The magnetic field  $\mu_0 H$  is applied parallel to the layers.

voltages a considerable magnetoresistance  $-\Delta\rho/\rho_0 = 60\%$  is seen for  $\mu_0 H = 1$  T; this vanishes at low applied voltages.

### C. Analysis of current-voltage characteristics

The current-voltage characteristics of the four CPP devices as well as of the in-plane bridge have been measured. The measurements were performed at constant temperature and field for increasing and decreasing voltages to exclude heating effects. A small difference between forward and reverse bias was seen in both the CPP and the CIP resistance. Since the  $I$ - $V$  curves for forward and reverse bias are qualitatively similar, only curves taken at forward bias are shown.

In Figs. 6(a) and 6(b) the  $I$ - $V$  curves in the CPP geometry of a Ti/La<sub>0.7</sub>Ca<sub>0.3</sub>MnO<sub>3</sub>/Ti trilayer, sample A, recorded in zero field and for 1 T are shown on a double logarithmic scale, respectively. The results are characteristic for all devices. In general the current-voltage characteristics are nonlinear with the nonlinearity increasing at low temperatures. The  $I$ - $V$  curves are best described by a simple power law

$$I \propto V^n \quad (4)$$

with a temperature and slightly field dependent exponent  $n$ . We find the values  $n = 1.120 \pm 0.004$  (300 K),  $n = 1.399 \pm 0.006$  (175 K), and  $n = 2.747 \pm 0.023$  (96 K) in zero field and  $n = 1.475 \pm 0.009$  (175 K) and  $n = 2.915 \pm 0.034$  (96 K) in a field of 1 T applied parallel to the layers. The theoretical value<sup>7</sup>  $n = 7/3$  for quasiparticle tunneling via pairs of localized states is intermediate to the measured values at 96 and 175 K.

The data do not fit an exponential form<sup>8</sup>

$$I = I_S [\exp(V/V_T) - 1] \quad (5)$$

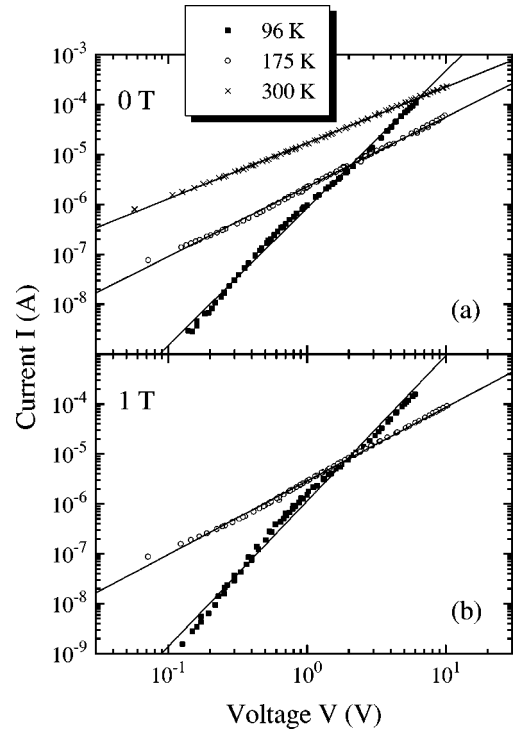


FIG. 6. Current-voltage curves of a Ti/La<sub>0.7</sub>Ca<sub>0.3</sub>MnO<sub>3</sub>/Ti heterostructure, sample A, at 96 K in (a) zero field and (b)  $\mu_0 H = 1$  T. The solid lines are least-square fits of a power law  $I \propto V^n$ , Eq. (4), to the data. The extracted values of the exponent  $n$  are  $1.120 \pm 0.004$  (300 K),  $1.399 \pm 0.006$  (175 K) and  $2.747 \pm 0.023$  (96 K) in zero field and  $1.475 \pm 0.009$  (175 K), and  $2.915 \pm 0.034$  (96 K) in a field of 1 T.

with  $V_T = kT/e$  as a simple model for a Schottky barrier. Therefore we conclude that the interface resistance is not due to Schottky barrier formation at the manganite/normal-metal interface but due to the formation of a highly resistive interface layer. This layer contains disordered magnetic impurities that scatter the quasiparticles. This interpretation is corroborated by the observation that the resistance after application and removal of a magnetic field  $B \leq 10$  mT increases logarithmically in time, thus indicating the presence of frustrated interfacial spins.

These findings are similar to the  $I$ - $V$  curves observed in YBa<sub>2</sub>Cu<sub>3</sub>O<sub>7</sub>/La<sub>0.7</sub>Ca<sub>0.3</sub>MnO<sub>3</sub>/YBa<sub>2</sub>Cu<sub>3</sub>O<sub>7</sub> trilayers<sup>9</sup> that have been interpreted as a proximity effect with a highly resistive interface formed at the superconductor-ferromagnet interface due to interdiffusion of Cu and Mn.<sup>1</sup> In recent work Bari *et al.*<sup>10</sup> report nonlinear current-voltage characteristics of epitaxial YBa<sub>2</sub>Cu<sub>3</sub>O<sub>7</sub>/La<sub>0.7</sub>Ca<sub>0.3</sub>MnO<sub>3</sub>/YBa<sub>2</sub>Cu<sub>3</sub>O<sub>7</sub> trilayers evidencing a high interface resistance. The  $I$ - $V$  curves of those heterostructures can be understood by inelastic tunneling via localized states. Bari *et al.*<sup>10</sup> propose that oxygen diffusion across the interface is a likely origin of the high interface resistivity.

In Fig. 7 the total resistance  $R = V/I$  of the in-plane bridge with two titanium contacts is shown. For better comparison the data were normalized by the resistance value in the zero current limit. At low currents the resistance shows a plateau and drops off at higher currents. The current dependence is stronger in the ferromagnetic state than in the normal state. From these measurements we conclude that both the

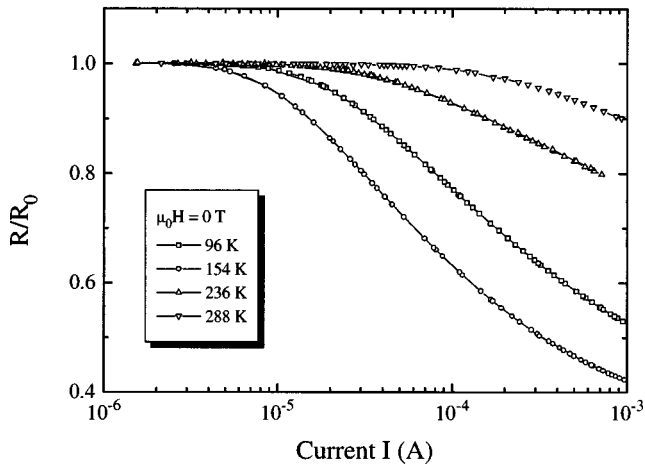


FIG. 7. CIP resistance of a  $\text{Ti/La}_{0.7}\text{Ca}_{0.3}\text{MnO}_3/\text{Ti}$  bridge in zero field normalized by the resistance value in the low current limit as a function of applied current. The normalization values are  $R_0 = 3.74 \text{ k}\Omega$  (96 K),  $9.30 \text{ k}\Omega$  (154 K),  $28.5 \text{ k}\Omega$  (236 K), and  $14.7 \text{ k}\Omega$  (288 K).

$\text{Ti/La}_{0.7}\text{Ca}_{0.3}\text{MnO}_3$  as well as the  $\text{TiO}_x/\text{La}_{0.7}\text{Ca}_{0.3}\text{MnO}_3$  interface contribute to the observed nonlinear CPP resistance. However, whereas the CIP resistance saturates at low currents the CPP resistance at low temperature does not show any sign of saturation down to  $10^{-9} \text{ A}$ , see Fig. 6. This finding might indicate that the boundary resistance mainly stems from the  $\text{TiO}_x/\text{La}_{0.7}\text{Ca}_{0.3}\text{MnO}_3$  interface. It might be due to interdiffusion of manganese and titanium or to oxygen diffusion from the  $\text{La}_{0.7}\text{Ca}_{0.3}\text{MnO}_3$  film into the titanium layer, thus leaving a thin oxygen depleted  $\text{La}_{0.7}\text{Ca}_{0.3}\text{MnO}_3$  layer at the interface.

#### IV. CONCLUSIONS

In this work the magnetoresistance of  $\text{La}_{0.7}\text{Ca}_{0.3}\text{MnO}_3/\text{normal-metal}$  multilayers has been investigated. We observe a colossal magnetoresistance in  $\text{Ti/La}_{0.7}\text{Ca}_{0.3}\text{MnO}_3/\text{Ti}$  and  $\text{Ti/Ni/La}_{0.7}\text{Ca}_{0.3}\text{MnO}_3/\text{Ti}$  heterostructures that is attributed to quasiparticle scattering by magnetic impurities in the interfaces. The application of high magnetic fields aligns the interfacial spins and reduces the magnetic scattering, thus yielding a colossal interfacial magnetoresistance. The boundary resistance might be caused by a disordered  $\text{TiO}_x/\text{La}_{0.7}\text{Ca}_{0.3}\text{MnO}_3$  interface due to titanium and manganese interdiffusion or the formation of an oxygen depleted layer in the  $\text{La}_{0.7}\text{Ca}_{0.3}\text{MnO}_3$  film. Due to the large magnitude of the interface resistance magnetoresistive effects in  $\text{Ti/Ni/La}_{0.7}\text{Ca}_{0.3}\text{MnO}_3/\text{Ti}$  multilayers related to spin polarized carrier injection from nickel into  $\text{La}_{0.7}\text{Ca}_{0.3}\text{MnO}_3$  are concealed.<sup>3,11</sup> We have investigated the magnetic properties of  $\text{La}_{0.7}\text{Ca}_{0.3}\text{MnO}_3/\text{permalloy}$  bilayers and did not find any exchange coupling. This result might indicate the formation of an interface containing frustrated spins. Ferromagnetic resonance measurements on  $\text{YBa}_2\text{Cu}_3\text{O}_7/\text{permalloy}$  bilayers yield similar results indicating a spin-glass-like interface layer.<sup>12</sup> To observe magnetoresistive effects due to spin polarized currents going from a classical ferromagnet into a ferromagnetic manganite the interface properties of manganite/normal-metal heterostructures have to be greatly improved. The CPP devices presented here show the unique feature of a voltage controlled colossal magnetoresistance.

#### ACKNOWLEDGMENT

This work was supported by the European Union TMR ‘‘OXSEN’’ network.

<sup>1</sup>J. M. D. Coey, M. Viret, and S. von Molnar, *Adv. Phys.* (to be published).  
<sup>2</sup>N. D. Mathur, G. Burnell, S. P. Isaac, T. J. Jackson, B. S. Teo, J. L. MacManus-Driscoll, L. F. Cohen, J. E. Evetts, and M. G. Blamire, *Nature* (London) **387**, 266 (1997); K. Steenbeck, T. Eick, K. Kirsch, K. O’Donnell, and E. Steinbeiß, *Appl. Phys. Lett.* **71**, 968 (1997).  
<sup>3</sup>M. R. J. Gibbs, M. Ziese, G. A. Gehring, H. J. Blythe, D. J. Coombes, S. P. Sena, and C. Shearwood, *Philos. Trans. R. Soc. London, Ser. A* (to be published).  
<sup>4</sup>H. Gruber and E. Krautz, *Phys. Status Solidi A* **69**, 287 (1982); **75**, 511 (1983).  
<sup>5</sup>W. P. Pratt, Jr., S.-F. Lee, J. M. Slaughter, R. Loloee, P. A. Schroeder, and J. Bass, *Phys. Rev. Lett.* **66**, 3060 (1991).

<sup>6</sup>G. J. Snyder, R. Hiskes, S. DiCarolis, M. R. Beasley, and T. H. Geballe, *Phys. Rev. B* **53**, 14 434 (1996).  
<sup>7</sup>L. I. Glazman and K. A. Matveev, *Zh. Éksp. Teor. Fiz.* **94**, 332 (1988) [*Sov. Phys. JETP* **67**, 1276 (1988)].  
<sup>8</sup>S. M. Sze, *Physics of Semiconductor Devices* (Wiley, New York, 1981), p. 245ff.  
<sup>9</sup>M. Kasai, Y. Kanke, T. Ohno, and Y. Kozono, *J. Appl. Phys.* **72**, 5344 (1992).  
<sup>10</sup>M. A. Bari, O. Cabeza, L. Capogna, P. Woodall, and C. M. Muirhead, *IEEE Trans. Appl. Supercond.* **7**, 2304 (1997).  
<sup>11</sup>D. J. Coombes and G. A. Gehring, *J. Magn. Magn. Mater.* (to be published).  
<sup>12</sup>M. Rubinstein, P. Lubitz, W. E. Carlos, P. R. Broussard, D. B. Chrisey, J. Horwitz, and J. J. Krebs, *Phys. Rev. B* **47**, 15 350 (1993).